AIP | The Journal of Chemical Physics

Peptide folding in the presence of interacting protein crowders

Anna Bille, Sandipan Mohanty, and Anders Irbäck

Citation: The Journal of Chemical Physics **144**, 175105 (2016); doi: 10.1063/1.4948462
View online: http://dx.doi.org/10.1063/1.4948462
View Table of Contents: http://scitation.aip.org/content/aip/journal/jcp/144/17?ver=pdfcov
Published by the AIP Publishing

Peptide folding in the presence of interacting protein crowders

Anna Bille,[1,a)] Sandipan Mohanty,[2,b)] and Anders Irbäck[1,c)]
[1]*Computational Biology and Biological Physics, Department of Astronomy and Theoretical Physics, Lund University, Sölvegatan 14A, SE-223 62 Lund, Sweden*
[2]*Jülich Supercomputing Centre, Institute for Advanced Simulation, Forschungszentrum Jülich, D-52425 Jülich, Germany*

(Received 4 March 2016; accepted 20 April 2016; published online 5 May 2016)

Using Monte Carlo methods, we explore and compare the effects of two protein crowders, BPTI and GB1, on the folding thermodynamics of two peptides, the compact helical trp-cage and the β-hairpin-forming GB1m3. The thermally highly stable crowder proteins are modeled using a fixed backbone and rotatable side-chains, whereas the peptides are free to fold and unfold. In the simulations, the crowder proteins tend to distort the trp-cage fold, while having a stabilizing effect on GB1m3. The extent of the effects on a given peptide depends on the crowder type. Due to a sticky patch on its surface, BPTI causes larger changes than GB1 in the melting properties of the peptides. The observed effects on the peptides stem largely from attractive and specific interactions with the crowder surfaces, and differ from those seen in reference simulations with purely steric crowder particles. *Published by AIP Publishing.* [http://dx.doi.org/10.1063/1.4948462]

I. INTRODUCTION

In the crowded interior of a cell, proteins are exposed to interactions with surrounding macromolecules. It is well established that purely steric effects tend to stabilize globular proteins.[1–3] However, in experiments using concentrated protein solutions or cells, both stabilization and destabilization of globular proteins have been observed, indicating that non-steric interactions play a significant role.[4–13] For a fundamental understanding of the combined effect of the interactions in these systems, there is a need for complementary computational approaches.

In this article, we present equilibrium Monte Carlo simulations of two structurally dissimilar peptides in the presence of protein crowders, performed using an all-atom protein model along with an implicit solvent force field.[14] Their malleability makes peptides interesting model systems for studying crowding effects. The peptides used in the present study are the compact α-helical trp-cage[15] and the β-hairpin-forming GB1m3,[16] with 20 and 16 residues, respectively. To test the dependence on crowder type, each peptide is simulated using two different crowding agents, namely the 58-residue bovine pancreatic trypsin inhibitor (BPTI) and the 56-residue B1 domain of streptococcal protein G (GB1). These proteins differ in terms of fold and physicochemical properties, but both are thermally highly stable.[17,18] In our calculations, the backbone degrees of freedom of the crowder molecules are kept fixed, whereas their side-chain as well as rigid body degrees of freedom are free to change. Our interaction potential does not treat the crowders in any special way. The crowders interact among themselves and with the test peptides with the full potential of the model, which includes both repulsive and attractive terms.

Recent years have seen the development of a variety of computational approaches for studying biomolecular processes and properties in crowded environments, including diffusion properties.[19–23] Simulations of processes involving protein conformational changes have so far focused mainly on steric effects, often using spherical crowder particles.[24–32] A computational scheme sometimes used, in place of direct simulation of the full system, is to insert simulated structures of the free protein of interest into separately generated crowder configurations, by reweighting techniques.[19,33,34] While this scheme, like the use of spherical crowders, can speed up the calculations, there remains a need for methods permitting direct simulation with macromolecular crowders, modeled in atomic detail. Pioneering simulations of this kind, based on molecular dynamics methods, have recently been reported.[8,35–38]

The present study focuses on crowder-induced changes in the equilibrium properties of our two peptides. The problem of determining folding/unfolding equilibria in the presence of the crowders is tackled by direct Monte Carlo-based simulation. The feasibility of this approach was recently demonstrated for one of the systems studied in the present article (trp-cage–BPTI).[39] Here, these methods are applied to four different systems, in order to compare the crowding response of two different peptides and test the dependence on crowder type.

II. METHODS

A. Simulated systems

The test peptides studied, trp-cage[15] and GB1m3,[16] are designed and thermally stable for their size, but much less stable than the proteins serving as crowding agents in our simulations, BPTI and GB1. Some basic properties of these peptides and proteins can be found in Table I. Their

a)Electronic mail: anna.bille@thep.lu.se
b)Electronic mail: s.mohanty@fz-juelich.de
c)Electronic mail: anders@thep.lu.se

TABLE I. Some basic properties of the peptides and proteins studied.

Name	PDB ID	No. of residues	Net charge	Melting temperature (°C)
trp-cage	1L2Y	20	+1	42 (Ref. 15)
GB1m3	...	16	+2	60 (Ref. 16)
BPTI	4PTI	58	+6	>100 (Ref. 17)
GB1	2GB1	56	−4	87 (Ref. 18)

native folds are illustrated in Figure 1. The GB1m3 peptide is an optimized variant of the second β-hairpin (residues 41–56) of protein GB1[40] with enhanced stability.[16] The two sequences differ at 7 of 16 positions. To our knowledge, no experimental structure is available for GB1m3, but its native fold is expected to be similar to the parent β-hairpin in GB1.

Each test peptide is simulated under four sets of conditions: (i) with GB1 crowders, (ii) with BPTI crowders, (iii) with hard-sphere crowders, and (iv) without crowders. In all simulations with crowders, the studied system consists of one test peptide and eight crowder entities, enclosed in a periodic box with side length 95 Å. This setup yields GB1 and BPTI crowder densities of ∼100 mg/ml, which is sufficient for noticeable effects to occur in the simulations. This density is slightly lower than estimated macromolecule densities in cells (∼300–400 mg/ml).[41] The volume fraction occupied by the GB1 and BPTI crowders is 7%.

B. Model

All simulations are performed using an all-atom protein representation with torsion angles as the degrees of freedom, and an implicit solvent force field.[14] A detailed description of the interaction potential can be found elsewhere.[14] In brief, the potential consists of four main terms, $E = E_{\rm loc} + E_{\rm ev} + E_{\rm hb} + E_{\rm sc}$. The first ($E_{\rm loc}$) represents local interactions between atoms separated by only a few covalent bonds. The other terms are non-local and represent excluded-volume effects ($E_{\rm ev}$), hydrogen bonding ($E_{\rm hb}$), and residue-specific interactions between pairs of side-chains, based on hydrophobicity and charge ($E_{\rm sc}$). This potential is an effective energy function, parameterized through folding thermodynamics studies for a structurally diverse set of peptides and small proteins, which contained trp-cage and GB1m3.[14] The model has been used, with unchanged parameters, to study folding/unfolding properties of proteins with >90 residues.[42–46] Other applications include peptide aggregation.[47,48] In multi-chain simulations, intermolecular energy terms have the same form and strength as the intramolecular ones. Hence, in our present simulations with protein crowders, the crowder molecules interact with each other and with the test peptides through a mixture of attractive and repulsive terms.

The same model was used in our previous study of trp-cage with BPTI crowders.[39] The minor numerical differences in the results presented below for the trp-cage–BPTI system, compared to those obtained in our earlier study,[39] are due to charges at the ends of the trp-cage chain. The figures shown in our previous publication[39] were made, inadvertently, from simulations without those charges, whereas the plots in this article are with the correct default treatment of those charges in our model. The presence or absence of these charges does not affect any conclusions drawn in the earlier article.[39]

Our simulations are performed using the same all-atom representation of both test peptides and crowder proteins. However, since both BPTI and GB1 are known to be thermally highly stable (Table I), crowder molecules are assumed to stay folded. They are modeled as having a fixed backbone but rotatable side-chains. The assumed backbone conformations of BPTI and GB1 are model approximations of the PDB structures 4PTI and 2GB1, respectively, derived by Monte Carlo with minimization. The structures were selected for both low energy and high similarity to the experimental structures. The root-mean-square deviations (RMSDs) from the experimental structures (calculated over backbone and C^β atoms) were $\lesssim$1 Å.

The BPTI fold contains three disulfide bonds, each of which is modeled using four harmonic distance restraints between the S and C^β atoms of the two cysteine residues involved. Equilibrium distances are taken from the crystal structure. The GB1 protein has no cysteines.

For comparison, we also perform simulations with abstract spherical crowders. The interaction energy between a spherical crowder with radius $\sigma_{\rm C}$ and a test peptide atom or another spherical crowder with radius σ_i at center-to-center distance r is zero if $r > \sigma_i + \sigma_{\rm C}$, and infinite otherwise. The hard-sphere radius is set to $\sigma_{\rm C} = 17.2$ Å, which roughly corresponds to the maximum diameter of our protein crowders. The volume fraction occupied by crowders is therefore higher

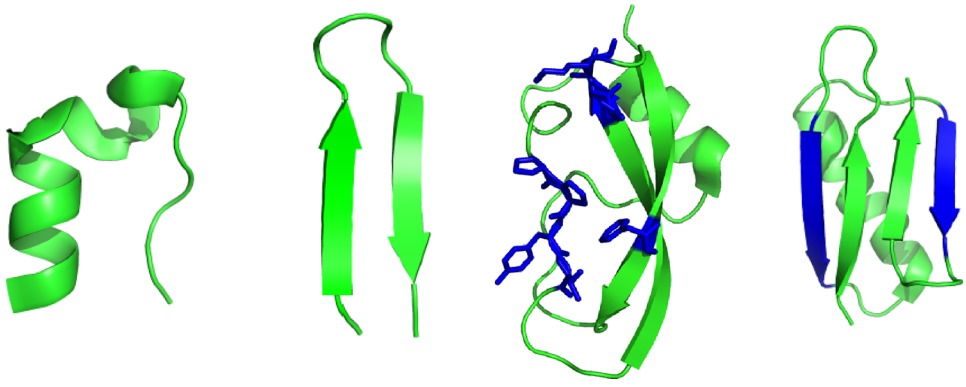

FIG. 1. Schematic illustration of the native folds of (from left to right) trp-cage (PDB ID 1L2Y), GB1m3, BPTI (4PTI), and GB1 (2GB1). In the BPTI fold, the residues Pro8, Pro9, Tyr10, Thr11, Asn24, Ala25, Lys26, and Phe33 are shown in stick representation and blue color. The GB1 fold contains a four-stranded β-sheet, whose edge strands β2 (residues 14–19) and β3 (42–46) are indicated in blue.

in our simulations with hard-sphere crowders (20%) than it is in those with protein crowders (7%). Despite their size, the effects of the hard-sphere crowders turn out be modest, compared to those of the protein crowders. With the same volume as for the protein crowders, the effects of the hard-sphere crowders would have been even smaller, as observed in our previous trp-cage–BPTI study.[39]

C. Monte Carlo details

The systems are simulated using Monte Carlo replica-exchange techniques,[49] with 16 temperatures geometrically distributed over a system-dependent interval. Our Monte Carlo move set is as described previously.[48] The simulations are started with the crowders placed in the corners of a virtual cube inside the simulation box, and with the test peptide at the center of this cube in a random conformation.

All calculations are done with the program PROFASI,[50] improved with both vector and thread parallelization to achieve the necessary performance. For each system, 10^7 sweeps per replica are generated, where one sweep consists of one attempted elementary update per degree of freedom. It was verified that this simulation length is sufficient to ensure reproducible results for the systems with protein crowders, which are by far the most challenging ones. Each of the systems with protein crowders required about two weeks of computing time using a total of 64 cores for the 16 replica in our replica-exchange procedure.

D. Analysis

To describe the effects caused by the crowders, several structural properties of the test peptides are monitored in the simulations. Secondary structure is analyzed using the program STRIDE.[51] The extension of the peptide chains is assessed using both the radius of gyration, R_g, calculated over all non-hydrogen atoms, and the end-to-end distance, R_{ee}, defined as the C^α–C^α distance between the end residues. The nativeness of trp-cage is measured using the backbone RMSD from the NMR structure (PDB ID 1L2Y), Δ. The two end residues are flexible and therefore omitted in the RMSD calculation. For GB1m3, the fraction of native hydrogen bonds present, q, serves as a nativeness measure. It is assumed that the native hydrogen bonds are as in the full GB1 protein (PDB ID 2GB1).

To characterize intermolecular interactions, residue-residue contact frequencies are measured. Two residues are defined to be in contact if their C^α atoms are within 8 Å from each other. The number of contacts that test peptide residue i forms with residues in position j in any of the crowder molecules is denoted by n_{ij}^{tc}. Similarly, n_{ij}^{cc} is the average number of contacts that residue i in an arbitrary given crowder molecule forms with residues in position j in any of the other crowder molecules. Ensemble averages of these matrices are visualized in contact maps. The total number of test peptide-crowder protein contacts is $n^{tc} = \sum_{ij} n_{ij}^{tc}$, and the average number of contacts between an arbitrary given crowder molecule and the other crowder molecules is $n^{cc} = \sum_{ij} n_{ij}^{cc}$.

III. RESULTS

A. Neither BPTI nor GB1 stabilizes trp-cage

We first examine the response of trp-cage to crowding. Figure 2 shows the temperature dependence of four structural properties of trp-cage under the different simulated conditions. The properties studied are the α-helix content, H, the radius of gyration, R_g, the RMSD, Δ, and the end-to-end distance, R_{ee} (see Sec. II).

The effects of the purely steric, spherical crowders are, as expected, largest at high temperatures (Figure 2), where the peptide is unfolded and requires the most volume. The presence of the crowders leads to a reduction of R_g, R_{ee}, and Δ, and therefore to an apparent stabilization of trp-cage. However, as the trp-cage molecule is small and unlikely to behave as an ideal two-state system, one may expect the precise response to depend on the observable studied. Such a dependence can indeed be seen in our simulations, as demonstrated by the data for H. Unlike the other three observables shown in Figure 2, H is left almost unchanged by the spherical crowders.

These results obtained with spherical crowders contrast sharply with what is found with BPTI or GB1 crowders (Figure 2). First, BPTI and GB1 are smaller than the spherical crowders and cause only marginal effects on trp-cage at high temperatures. Second, at low temperatures, BPTI and GB1 tend to decrease the nativeness of trp-cage, whereas the spherical crowders have a weakly stabilizing effect.

The distorting effect of GB1 is weak, with noticeable but small changes in all four trp-cage properties studied, at low temperatures (Figure 2). Figure 3 shows the folding free energies $F(R_g, R_{ee})$ and $F(R_g, \Delta)$ of trp-cage, in isolation and in the presence of GB1 crowders, at 290 K. The free energies show that the GB1-induced changes in these quantities are small, not only at the level of thermal averages. The trp-cage–GB1 system has previously been studied by Predeus *et al.*,[36] using mixed resolution (all-atom peptide/coarse-grained crowders/implicit solvent) molecular dynamics simulations. With GB1 crowders, they observed a set of partially unfolded trp-cage states, which were not sampled in reference simulations without crowders. In our simulations, rather than stabilizing a few specific states, GB1 causes many small shifts in the conformational ensemble of trp-cage (Figure 3). Our conclusion that the overall effects of GB1 on trp-cage are small and destabilizing in nature is, however, in good agreement with the findings of Predeus *et al.*[36]

Of our three crowding agents, BPTI is the one with largest impact on trp-cage. At intermediate temperatures (310 K $\lesssim T \lesssim$ 340 K), the BPTI crowders have an apparent stabilizing effect on trp-cage, as judged from an increase in H and decreases in both R_g and Δ. The shifts are larger than with spherical crowders, and must in large part be caused by attractive interactions, rather than by steric interactions alone. These interactions become even more important at low temperatures, where they compete with the forces driving folding. In our simulations, the interaction with the BPTI crowders prevents trp-cage from adopting its native fold, as can be most clearly seen from the R_{ee} data. The C-terminal tail of trp-cage does not pack against the N-terminal α-helix, as it does in the native fold, and, as a result, R_{ee}

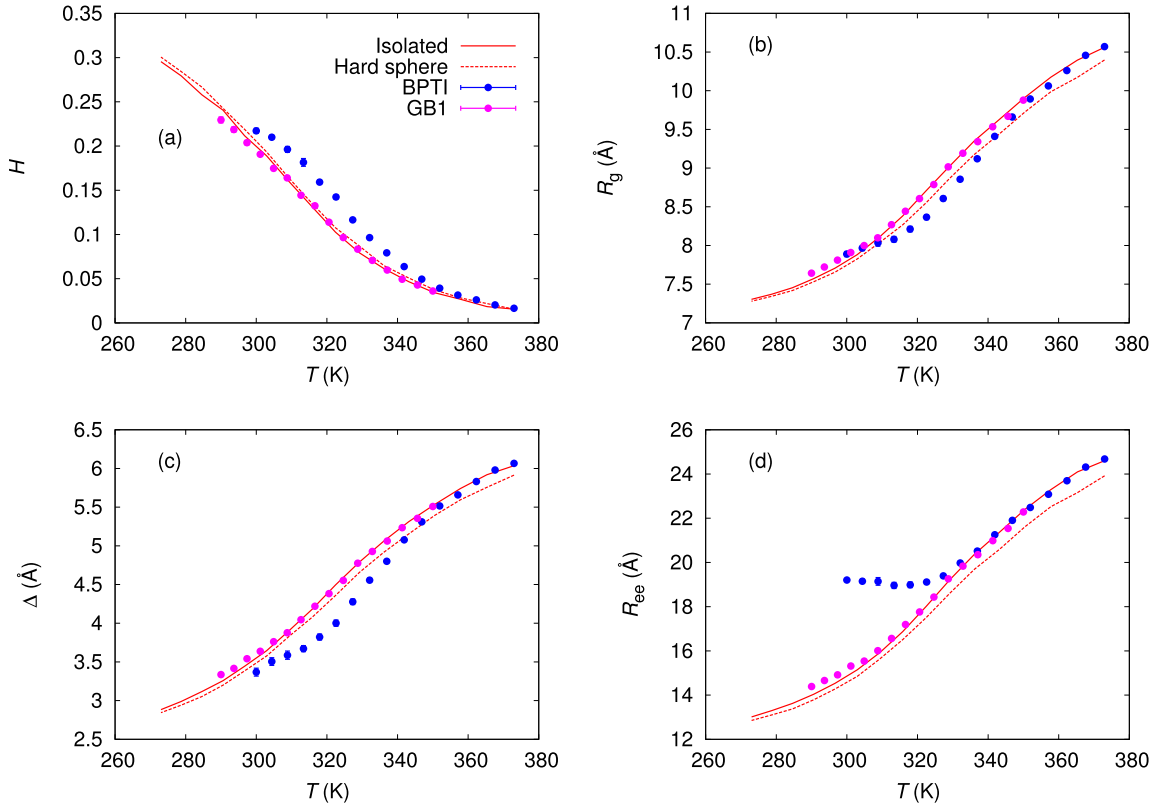

FIG. 2. Temperature dependence of structural properties of trp-cage in simulations without crowders (red line), with spherical crowders (red dashes), with BPTI crowders (blue symbols), and with GB1 crowders (purple symbols). The properties shown are (a) the helix content, H, (b) the radius of gyration, R_g, (c) the backbone RMSD, Δ, and (d) the end-to-end distance, R_{ee}. Secondary structure is assigned using STRIDE.[51] For the simulations without crowders and those with spherical crowders, the statistical uncertainties are small and have been omitted for clarity.

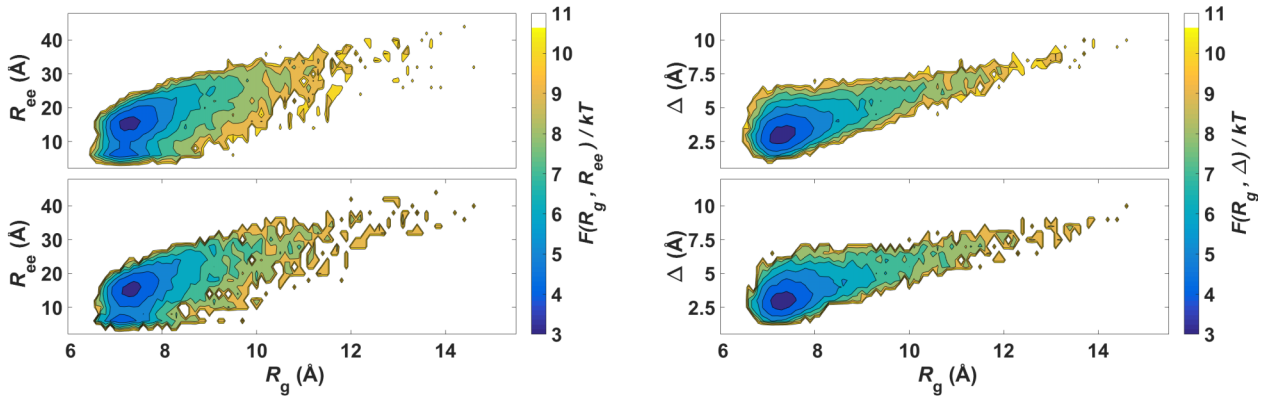

FIG. 3. Folding free energies of trp-cage in free form (upper panels) and in the presence of GB1 crowders (lower panels), at 290 K. Left panels show the free energy $F(R_g, R_{ee})$, calculated as a function of the radius of gyration and the end-to-end distance. Right panels show $F(R_g, Δ)$, where Δ is the RMSD from the native structure.

stays high at low temperatures. A more detailed view of this conformational distortion of trp-cage is provided by the free energies $F(R_g, R_{ee})$ and $F(R_g, Δ)$. While being left almost unchanged by GB1 (Figure 3), these free energies undergo some noticeable changes when BPTI is added (Figure 4). In addition to an expected upward shift of the minimum of $F(R_g, R_{ee})$ (compare Figure 2), BPTI is seen to cause a suppression of expanded high-R_g states.

Figure 5 compares residue-specific α-helix probabilities of trp-cage under the four sets of conditions. All four profiles are calculated at the melting temperature of the free peptide, 315 K.[15] In particular, this comparison shows that the BPTI-induced increase in overall helix content at intermediate temperatures (Figure 2(a)) stems from a stabilization of the native α-helix, rather than from the formation of non-native helix structure. A stabilization of the native α-helix is observed with spherical and GB1 crowders as well at this temperature, but the effect is much weaker than it is with BPTI crowders (Figure 5).

B. Both BPTI and GB1 stabilize GB1m3

We now turn to the effects of the same three crowders on the β-hairpin-forming GB1m3 peptide. Figure 6 illustrates

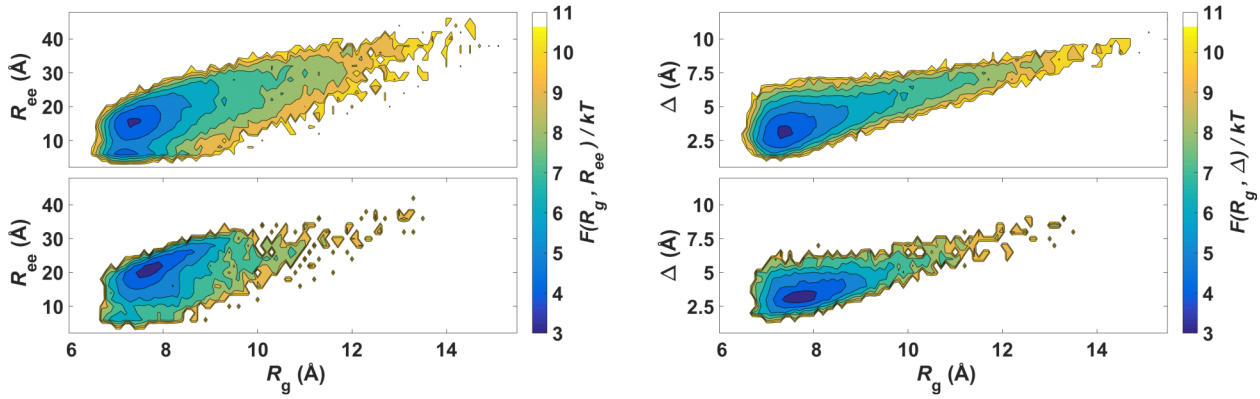

FIG. 4. Folding free energies of trp-cage in free form (upper panels) and in the presence of BPTI crowders (lower panels), at 300 K. Left panels show the free energy $F(R_g, R_{ee})$, calculated as a function of the radius of gyration and the end-to-end distance. Right panels show $F(R_g, \Delta)$, where Δ is the RMSD from the native structure.

the melting behavior of GB1m3 in the different simulated environments. The calculated properties are the strand content, S, the radius of gyration, R_g, the nativeness, q, and the end-to-end distance, R_{ee} (see Sec. II).

The spherical crowders give rise to a stabilization of GB1m3 (Figure 6), similar to that observed above for trp-cage. As in the trp-cage case, the exact magnitude of the crowding effects is observable-dependent. The R_g and R_{ee} data show that the spherical crowders cause a compaction of GB1m3 at high temperatures, whereas the secondary-structure content remains essentially unchanged over the entire temperature range.

The effects of the two protein crowders on GB1m3 are, by contrast, markedly different from what was observed above for trp-cage. First of all, at low temperatures, GB1m3 stays native-like in the presence of the crowders. The crowders modify the exact shape of the β-hairpin which, for instance, is made more planar by the interaction with GB1, as reflected in an increased R_g. However, the core of the β-hairpin, defined by its hydrogen bonds, is not altered by the crowders, as shown by the nativeness q. In fact, the fold is thermally stabilized by the crowders. The size of this effect is modest in the case of GB1, whereas BPTI causes shifts of the melting curves that correspond to an increase in midpoint temperature by as much as roughly 15 K.

That GB1m3 stays native-like in the presence of the crowders is further illustrated by residue-specific secondary-structure data. Figure 7 shows β-strand probability profiles of GB1m3 in the different systems, all calculated at the melting temperature of the free peptide, 333 K.[16] The β-strand-forming residues are indeed the same (2–6 and 11–15) in all four cases. When it comes to β-hairpin population, the BPTI system stands out from the other three. The β-strand probabilities are essentially twice as large in this system, compared to the other three.

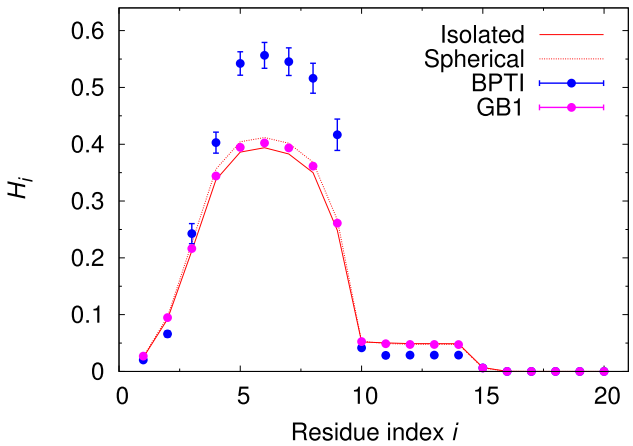

FIG. 5. Residue-specific α-helix probabilities, H_i, for trp-cage at $T = 315$ K, as obtained without crowders (red line), with spherical crowders (red dashes), with BPTI crowders (blue symbols), and with GB1 crowders (purple symbols). Secondary structure is assigned using STRIDE.[51] Without crowders or with spherical crowders, the statistical uncertainties are small and are, for clarity, omitted.

C. Modes of interaction between the test peptides and the crowder proteins

Having studied the structural changes of the test peptides caused by the crowder proteins, we next look into the interactions mediating these effects. To this end, residue-residue contact maps are computed (see Sec. II) at the melting temperature of the free peptides, where a broad range of conformations is sampled. The contact maps immediately show that the test peptide-crowder protein interactions are not random (Figure 8). On the crowder surfaces, there are hotspot regions that are responsible for most of the contacts with the test peptides. In BPTI, the residues Pro8, Pro9, Tyr10, Thr11, Asn24, Ala25, Lys26, and Phe33 form a partly hydrophobic surface patch (Figure 1), which plays a dominant role in the interaction with the test peptides. Particularly interaction-prone are residues 8 and 9, both of which are prolines, which is striking but not entirely surprising. In fact, proline is known to play a special role in protein-protein interactions,[52] which is linked to its unique geometry. The interaction of GB1 with the test peptides is somewhat less specific in character. Still, just as for BPTI, there are large variations in interaction propensity on the surface of GB1, as is illustrated by its four-stranded β-sheet (Figure 1). The edge strands β2 (residues 14–19) and β3 (42–46) are much more prone than the inner strands

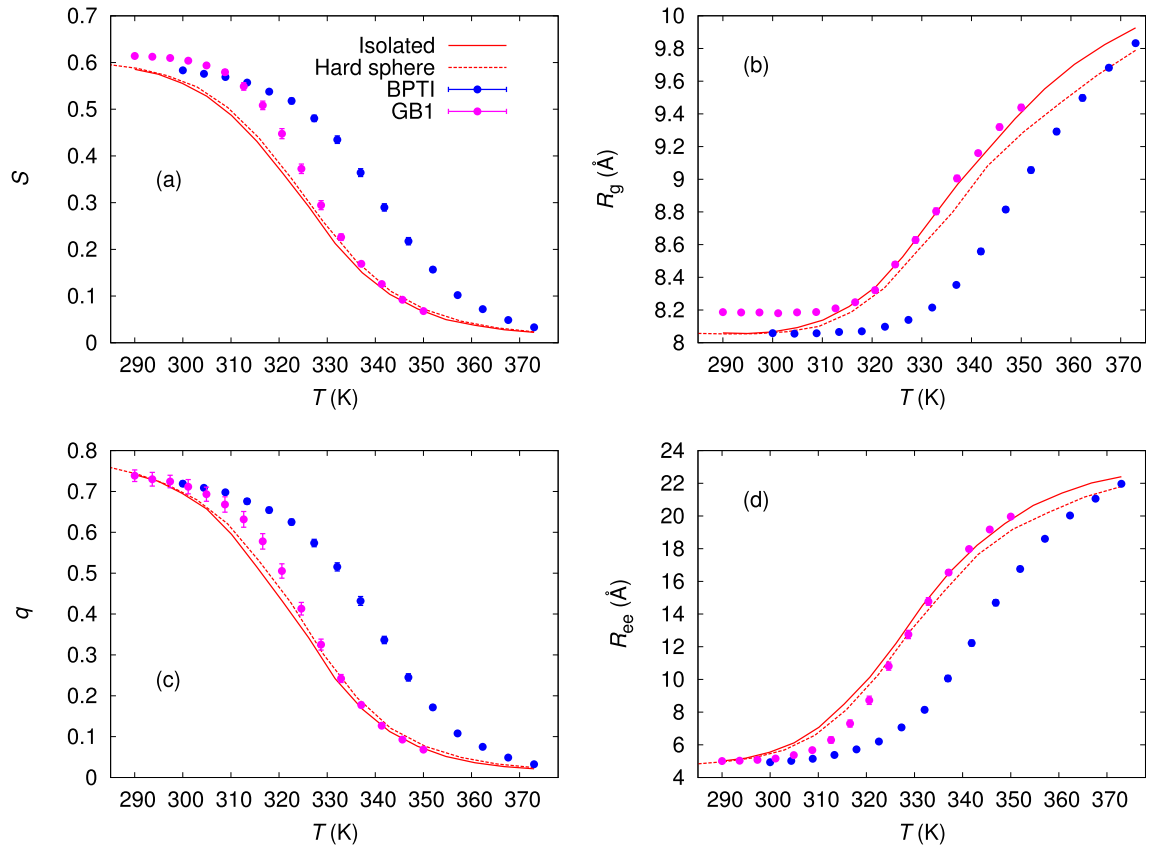

FIG. 6. Temperature dependence of structural properties of GB1m3 in simulations without crowders (red line), with spherical crowders (red dashes), with BPTI crowders (blue symbols), and with GB1 crowders (purple symbols). The properties shown are (a) the strand content, S, (b) the radius of gyration, R_g, (c) the nativeness, q, and (d) the end-to-end distance, R_{ee}. Secondary structure is assigned using STRIDE.[51] Without crowders or with spherical crowders, the statistical uncertainties are small and are, for clarity, omitted.

$\beta 1$ (2–7) and $\beta 4$ (51–55) to form contacts with the test peptides.

In the trp-cage–BPTI system, the above-mentioned patch on the BPTI surface interacts primarily with the C-terminal tail of trp-cage (Figure 8, left upper panel). The anchoring of this tail to BPTI has a stabilizing effect on the native α-helix (Figure 5). At the same time, it prevents a tight packing of the C-terminal tail against the α-helix, which leads to a large end-to-end distance (Figure 2(d)). A snapshot from the trp-cage–BPTI simulation can be found in Figure 9 (left panel).

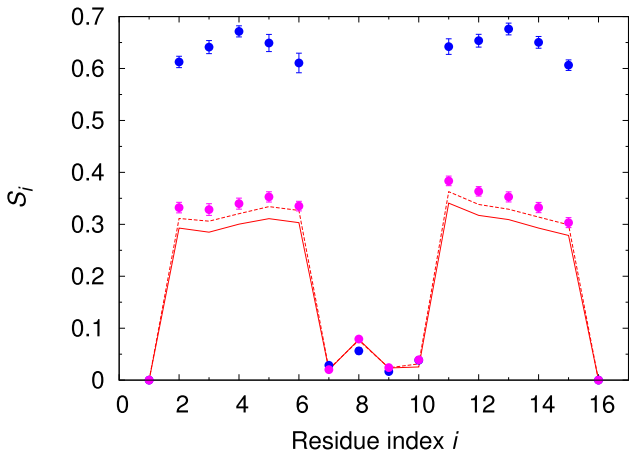

FIG. 7. Residue-specific β-strand probabilities, S_i, for GB1m3 at 333 K, as obtained without crowders (red line), with spherical crowders (red dashes), with BPTI crowders (blue symbols), and with GB1 crowders (purple symbols). Secondary structure is assigned using STRIDE.[51] Without crowders or with spherical crowders, the statistical uncertainties are small and are, for clarity, omitted.

Consistent with the results in Figure 2, the trp-cage–GB1 residue contact probabilities are generally low (Figure 8, left lower panel). There is some tendency for the N-terminal tail of trp-cage to transiently align, in an antiparallel fashion, to either the $\beta 3$ strand or a sequence segment containing the beginning of $\beta 2$. However, the frequency with which these contact patterns are observed is at most a few per cent.

In the GB1m3-BPTI interaction (Figure 8, right upper panel), which has a pronounced stabilizing effect on GB1m3 (Figure 6), a key role is played by the same set of BPTI residues that dominates its interaction with trp-cage. Most interaction-prone is Pro8, which interacts with both strands of the GB1m3 β-hairpin.

The GB1m3-GB1 interaction is special in that GB1m3 is related to the $\beta 3$-$\beta 4$ hairpin in GB1. In our simulations, the part of GB1 most prone to interact with GB1m3 is indeed the edge strand $\beta 3$ (Figure 8, right lower panel). The native state of GB1m3 contains a hydrophobic cluster, formed by the side-chains of Trp3, Tyr5, Phe12, and Val14. In its native state, GB1m3 can align side-by-side with the $\beta 3$ strand of GB1 in four ways to form an extended β-sheet, of which two are

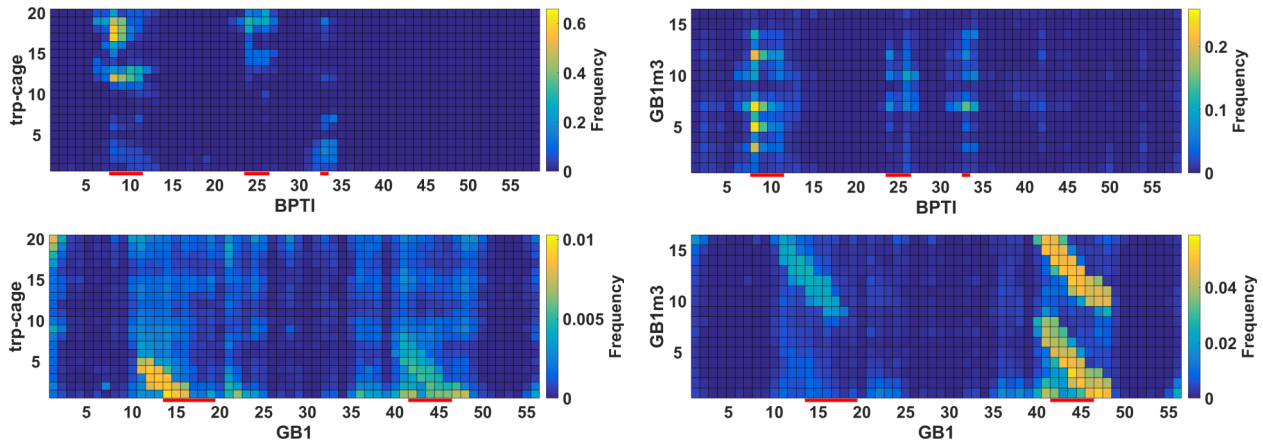

FIG. 8. Test peptide–crowder protein residue contact maps for our four simulated systems: trp-cage–BPTI (left upper panel), trp-cage–GB1 (left lower panel), GB1m3–BPTI (right upper panel), and GB1m3–GB1 (right lower panel). The temperature used is 315 K and 333 K for the trp-cage and GB1m3 systems, respectively. The indicated value for a given residue index pair (i, j) is the average number of C^{α}–C^{α} contacts between residue j in the test peptide and residue i in any of the eight crowder molecules, n_{ij}^{tc}. Red lines along the x axes indicate the positions of the residues Pro8, Pro9, Tyr10, Thr11, Asn24, Lys26, and Phe33 in BPTI, and the positions of the edge strands β2 (residues 14–19) and β3 (42–46) in GB1. Note the differences in scale between the panels. The contact cutoff distance is 8 Å.

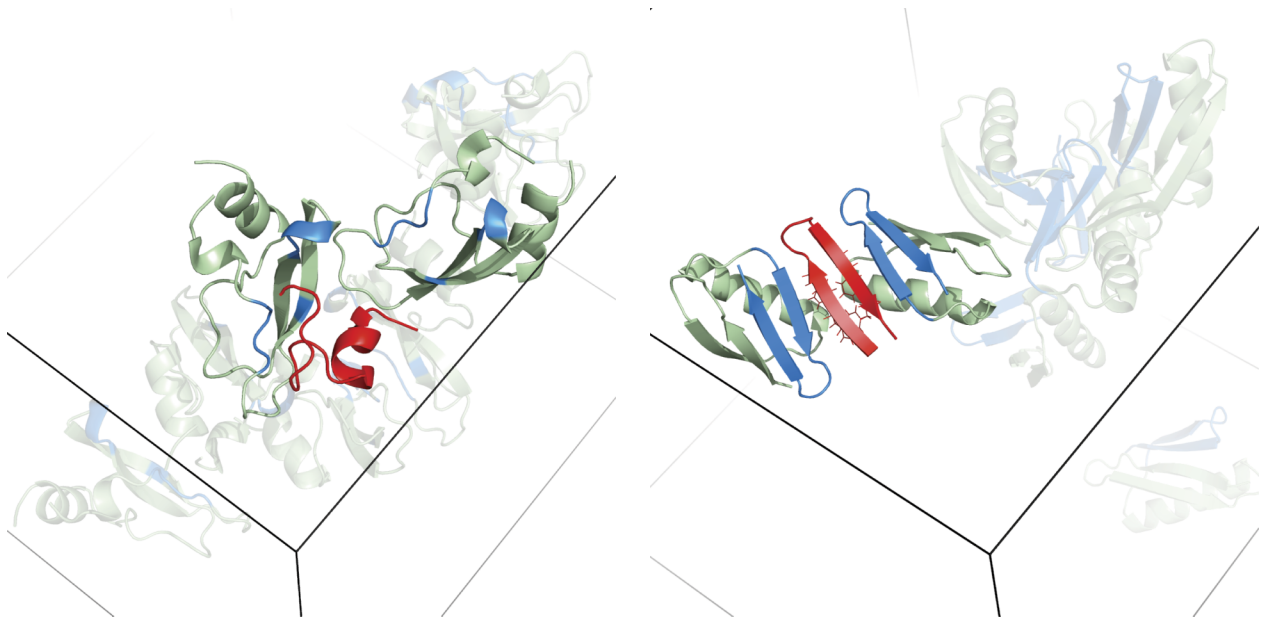

FIG. 9. Snapshots exhibiting salient interaction modes discussed in the text. Crowders are in pale green, test peptides are in red. For clarity, all crowders except the two nearest to the test peptides are shown faded. Left: trp-cage–BPTI. In the BPTI molecules, the same residues as in Figure 1 are colored blue, to emphasize their role in the interactions. Right: GB1m3-GB1. The C-terminal hairpin of the GB1 molecules are shown in blue. The hydrophobic side chains of residues Trp3, Tyr5, Phe12, and Val14 of GB1m3 can be seen (lines) facing toward the two interacting crowder GB1 molecules.

observed in our simulations (Figure 8, right lower panel). The observed relative orientations are such that the hydrophobic cluster of GB1m3 ends up on the same side of the extended β-sheet as the corresponding cluster in GB1 (Trp43, Tyr45, Phe52, and Val54). Figure 9 (right panel) shows a snapshot from the simulations, in which GB1m3 binds to two GB1 molecules. Together, the three molecules form a 10-stranded β-sheet.

D. The overall amount of test peptide-crowder protein interaction

The above contact map analysis was, for simplicity, restricted to a single temperature, the melting temperature of the free peptides, but the amount of test peptide-crowder protein interaction depends, of course, on temperature. To assess this dependence, the total number of test peptide-crowder protein residue contacts in the system, n^{tc}, is computed as a function of temperature (Figure 10). In three of four systems, this quantity increases in a gradual fashion with decreasing temperature. In the fourth system, GB1m3-GB1, n^{tc} shows a sigmoidal temperature dependence, indicating a cooperative, more sudden onset of test peptide-crowder protein binding.

In this system, the onset of binding occurs below the melting temperature of the free peptide (333 K), indicating that GB1m3 needs to fold first in order to bind efficiently to GB1. It can then bind to and extend the β-sheet of GB1.

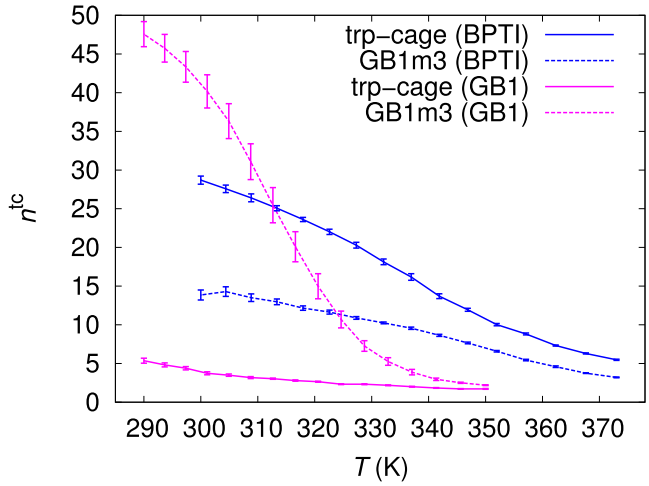

FIG. 10. Temperature dependence of the total number of test peptide-crowder protein residue contacts, n^{tc}, in the trp-cage–BPTI, trp-cage–GB1, GB1m3-BPTI, and GB1m3-GB1 systems. Each system consists of one test peptide (trp-cage or GB1m3) and eight crowder molecules (BPTI or GB1). The contact cutoff distance is 8 Å.

The native-like character of GB1m3 at low temperatures, where it is bound to GB1, is confirmed by our earlier analysis (Figure 6).

E. Self-interaction of the crowder proteins

A similar analysis of crowder-crowder contacts reveals that, in our simulations, BPTI and GB1 differ not only in their effects on the test peptides, but also in their propensity to self-interact. As an indicator of the amount of self-interaction, the average number of residue contacts between an arbitrary given crowder molecule and the other seven in the system, n^{cc}, is calculated. Figure 11 shows the temperature dependence of n^{cc}, as obtained using our four test peptide-crowder protein combinations. A first observation from this figure is that curves corresponding to the same crowder protein, but different test peptides, are similar. The amount of crowder-crowder contacts thus depends only weakly on the choice of test peptide, although the number of crowder molecules is not very large. Curves corresponding to different crowder proteins are, by contrast, far apart.

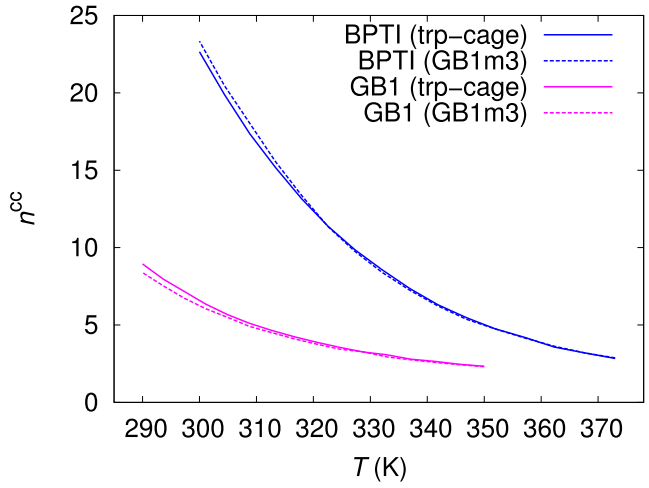

FIG. 11. Temperature dependence of the crowder-crowder contact number n^{cc} in the trp-cage–BPTI, trp-cage–GB1, GB1m3-BPTI, and GB1m3-GB1 systems. Each system consists of one test peptide (trp-cage or GB1m3) and eight crowder molecules (BPTI or GB1). Specifically, n^{cc} is defined as the average number of residue contacts between an arbitrary given crowder molecule and the other seven in the system. For clarity, error bars are omitted. The contact cutoff distance is 8 Å.

The data in Figure 11 show that BPTI is much more prone than GB1 to self-interact. As the temperature is reduced, the amount of contacts increases, due to attractive crowder-crowder interactions. The strong self-interaction of BPTI is in large part caused by the same surface region that dominates its interaction with the test peptides. The relatively weak self-interaction of GB1 may seem somewhat surprising, given the character and strength of its interaction with GB1m3 (Figures 8 and 10). As noted above, the GB1-bound form of GB1m3 is native-like and therefore structurally similar to the related β3-β4 hairpin in GB1. If sterically allowed, it should be possible for two GB1 molecules to interact in a similarly favorable way. However, inspection suggests that the bulkiness of GB1 prevents the formation of the favorable contacts that would be required for efficient self-interaction.

The residue-residue contacts formed by a given crowder tend to involve only one or a few of the other crowders in the system. To illustrate this, consider the trp-cage–BPTI and GB1m3-BPTI systems at 320 K, where $n^{cc} = 12.4$ (Figure 11). The average number of other crowders with which a given crowder forms at least one residue-residue contact is 1.1 in both these systems. A typical molecule-molecule contact thus involves many residue-residue contacts.

IV. DISCUSSION AND SUMMARY

Using atomic-level Monte Carlo simulations, we have in this article explored the effects of two thermally stable crowder proteins, BPTI and GB1, on the folding thermodynamics of two peptides, trp-cage and GB1m3. The observed crowding effects vary in extent and nature between the systems studied. Nevertheless, when comparing the results obtained for the four systems, some patterns emerge. Our main observations are as follows.

First, the peptides respond differently to the protein crowders. Both crowder proteins distort the native fold of trp-cage, while having a stabilizing effect on GB1m3. In the simulations, the native fold of GB1m3 is able to accommodate small adjustments that may be needed in order for the peptide to interact efficiently with the crowders. The free-energy barrier protecting the β-hairpin fold arises to a large part from cooperative formation of its hydrogen bonds.

Second, of the two crowder proteins, BPTI shows a generally higher propensity to interact intermolecularly, due to a sticky surface patch, containing the residues Pro8 and Pro9. Compared to BPTI, GB1 is less prone to self-interact and causes smaller changes in the melting properties of the peptides. It is worth noting, however, that GB1 interacts strongly with GB1m3 at low temperatures, where GB1m3, in native-like form, can bind to and extend the β-sheet of GB1.

Third, in all four systems, the observed effects on the peptides stem, in large part, from attractive interactions with the crowder proteins. The effects differ, in all four cases, from those seen in reference simulations with purely steric crowders.

These observations point to a few basic properties of the individual molecules as playing a key role in the simulated systems, such as the robustness of the GB1m3 fold and the sticky surface region of BPTI.

The trp-cage–GB1 system has previously been studied by Predeus *et al.*,[36] using molecular dynamics and a different model. The details of our computed free-energy landscapes for trp-cage (Figure 3) are not in perfect agreement with their results, although the statistical uncertainties are difficult to assess. However, at an overall level, our conclusions that the effects of GB1 on trp-cage are relatively weak and destabilizing in character agree well with their findings. Another similarity is that many observed trp-cage–GB1 contacts, in both our and their simulations, involve GB1 residues located at the β-sheet edges.

The systems studied in this article are in part chosen for computational tractability. Their equilibrium behavior can be investigated by direct simulation in a statistically controlled manner. Previous work shows that our model quite well captures the experimentally observed melting properties of trp-cage and GB1m3 in free form.[14] To our knowledge, there are not yet any experimental data available on the response of these peptides to macromolecular crowding.

The self-interaction of BPTI has been probed by two recent SAXS experiments.[53,54] The measured structure factors showed deviations from simple hard-sphere behavior. One study further found that, considering the asymmetric charge distribution on the BPTI surface, these deviations could be accounted for by screened electrostatic interactions.[54] In our simulations, the self-interaction of BPTI is strong (Figure 11), largely because of the sticky surface region containing Pro8 and Pro9. It would be interesting to test whether this interaction mechanism is consistent with experimental structure factors, but this would require simulations of larger systems and is beyond the scope of the present article.

ACKNOWLEDGMENTS

This work was in part supported by the Swedish Research Council (Grant No. 621-2014-4522). The simulations were performed on resources provided by the Swedish National Infrastructure for Computing (SNIC) at LUNARC, Lund University, Sweden, and Jülich Supercomputing Centre, Forschungszentrum Jülich, Germany.

[1]H.-X. Zhou, G. Rivas, and A. P. Minton, Annu. Rev. Biophys. **37**, 375 (2008).
[2]M. S. Cheung, D. Klimov, and D. Thirumalai, Proc. Natl. Acad. Sci. U. S. A. **102**, 4753 (2005).
[3]L. Stagg, S. Q. Zhang, M. S. Cheung, and P. Wittung-Stafshede, Proc. Natl. Acad. Sci. U. S. A. **104**, 18976 (2007).
[4]Z. Ignatova, B. Krishnan, J. P. Bombardier, A. M. C. Marcelino, J. Hong, and L. M. Gierasch, Biopolymers **88**, 157 (2007).
[5]K. Inomata, A. Ohno, H. Tochio, S. Isogai, T. Tenno, I. Nakase, T. Takeuchi, S. Futaki, Y. Ito, H. Hiroaki, and M. Shirakawa, Nature **458**, 106 (2009).
[6]S. Ebbinghaus, A. Dhar, J. D. McDonald, and M. Gruebele, Nat. Methods **7**, 319 (2010).
[7]J. Danielsson, K. Inomata, S. Murayama, H. Tochio, L. Lang, M. Shirakawa, and M. Oliveberg, J. Am. Chem. Soc. **135**, 10266 (2013).
[8]R. Harada, N. Tochio, T. Kigawa, Y. Sugita, and M. Feig, J. Am. Chem. Soc. **135**, 3696 (2013).
[9]W. B. Monteith and G. J. Pielak, Proc. Natl. Acad. Sci. U. S. A. **111**, 11335 (2014).
[10]I. Guzman, H. Gelman, J. Tai, and M. Gruebele, J. Mol. Biol. **426**, 11 (2014).
[11]W. B. Monteith, R. D. Cohen, A. E. Smith, E. Guzman-Cisneros, and G. J. Pielak, Proc. Natl. Acad. Sci. U. S. A. **112**, 1739 (2015).
[12]J. Danielsson, X. Mu, L. Lang, H. Wang, A. Binolfi, F.-X. Theillet, B. Bekei, D. T. Logan, P. Selenko, H. Wennerström, and M. Oliveberg, Proc. Natl. Acad. Sci. U. S. A. **112**, 12402 (2015).
[13]A. E. Smith, L. Z. Zhou, A. H. Gorensek, M. Senske, and G. J. Pielak, Proc. Natl. Acad. Sci. U. S. A. **113**, 1725 (2016).
[14]A. Irbäck, S. Mitternacht, and S. Mohanty, BMC Biophys. **2**, 2 (2009).
[15]J. W. Neidigh, R. M. Fesinmeyer, and N. H. Andersen, Nat. Struct. Biol. **9**, 425 (2002).
[16]R. M. Fesinmeyer, F. M. Hudson, and N. H. Andersen, J. Am. Chem. Soc. **126**, 7238 (2004).
[17]E. Moses and H.-J. Hinz, J. Mol. Biol. **170**, 765 (1983).
[18]A. M. Gronenborn, D. R. Filpula, N. Z. Essig, A. Achari, M. Whitlow, P. T. Wingfield, and G. M. Clore, Science **253**, 657 (1991).
[19]S. R. McGuffee and A. H. Elcock, PLoS Comput. Biol. **6**, e1000694 (2010).
[20]T. Ando and J. Skolnick, Proc. Natl. Acad. Sci. U. S. A. **107**, 18457 (2010).
[21]B. P. Cossins, M. P. Jacobson, and V. Guallar, PLoS Comput. Biol. **7**, e1002066 (2011).
[22]J. Balbo, P. Mereghetti, D.-P. Herten, and R. C. Wade, Biophys. J. **104**, 1576 (2013).
[23]F. Trovato and V. Tozzini, Biophys. J. **107**, 2579 (2014).
[24]D. D. L. Minh, C.-e. Chang, J. Trylska, V. Tozzini, and J. A. McCammon, J. Am. Chem. Soc. **128**, 6006 (2006).
[25]S. Qin and H.-X. Zhou, Biophys. J. **97**, 12 (2009).
[26]J. Mittal and R. B. Best, Biophys. J. **98**, 315 (2010).
[27]D. Tsao and N. V. Dokholyan, Phys. Chem. Chem. Phys. **12**, 3491 (2010).
[28]A. Samiotakis and M. S. Cheung, J. Chem. Phys. **135**, 175101 (2011).
[29]Q. Wang and M. S. Cheung, Biophys. J. **102**, 2353 (2012).
[30]S. Qin and H.-X. Zhou, J. Phys. Chem. Lett. **4**, 3429 (2013).
[31]D. C. Latshaw II and C. K. Hall, Biophys. J. **109**, 124 (2015).
[32]H. Kang, P. A. Pincus, C. Hyeon, and D. Thirumalai, Phys. Rev. Lett. **114**, 068303 (2015).
[33]S. Qin, D. D. L. Minh, J. A. McCammon, and H.-X. Zhou, J. Phys. Chem. Lett. **1**, 107 (2010).
[34]S. Qin, J. Mittal, and H.-X. Zhou, Phys. Biol. **10**, 045001 (2013).
[35]M. Feig and Y. Sugita, J. Phys. Chem. B **116**, 599 (2012).
[36]A. V. Predeus, S. Gul, S. M. Gopal, and M. Feig, J. Phys. Chem. B **116**, 8610 (2012).
[37]B. Macdonald, S. McCarley, S. Noeen, and A. E. van Giessen, J. Phys. Chem. B **119**, 2956 (2015).
[38]B. Macdonald, S. McCarley, S. Noeen, and A. E. van Giessen, J. Phys. Chem. B **120**, 650 (2016).
[39]A. Bille, B. Linse, S. Mohanty, and A. Irbäck, J. Chem. Phys. **143**, 175102 (2015).
[40]F. J. Blanco, G. Rivas, and L. Serrano, Nat. Struct. Mol. Biol. **1**, 584 (1994).
[41]A. Vendeville, D. Larivière, and E. Fourmentin, FEMS Microbiol. Rev. **35**, 395 (2011).
[42]S. Æ. Jónsson, S. Mohanty, and A. Irbäck, Proteins **80**, 2169 (2012).
[43]S. Mohanty, J. H. Meinke, and O. Zimmermann, Proteins **81**, 1446 (2013).
[44]A. Bille, S. Æ. Jónsson, M. Akke, and A. Irbäck, J. Phys. Chem. B **117**, 9194 (2013).
[45]S. A. Jónsson, S. Mitternacht, and A. Irbäck, Biophys. J. **104**, 2725 (2013).
[46]J. Petrlova, A. Bhattacherjee, W. Boomsma, S. Wallin, J. O. Lagerstedt, and A. Irbäck, Protein Sci. **23**, 1559 (2014).
[47]D. Li, S. Mohanty, A. Irbäck, and S. Huo, PLoS Comput. Biol. **4**, e1000238 (2008).
[48]S. Mitternacht, I. Staneva, T. Härd, and A. Irbäck, J. Mol. Biol. **410**, 357 (2011).
[49]R. H. Swendsen and J. S. Wang, Phys. Rev. Lett. **57**, 2607 (1986).
[50]A. Irbäck and S. Mohanty, J. Comput. Chem. **27**, 1548 (2006).
[51]D. Frishman and P. Argos, Proteins **23**, 566 (1995).
[52]B. K. Kay, M. P. Williamson, and M. Sudol, FASEB J. **14**, 231 (2000), available at http://www.fasebj.org/content/14/2/231.abstract.
[53]D. P. Goldenberg and B. Argyle, Biophys. J. **106**, 895 (2014).
[54]S. Kaieda, M. Lund, T. S. Plivelic, and B. Halle, J. Phys. Chem. B **118**, 10111 (2014).